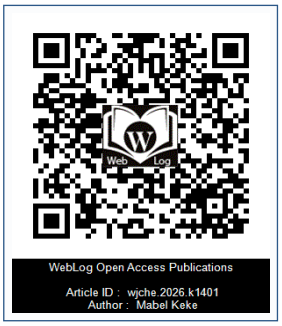
WebLog Journal of Chemical Engineering

Research Article
Published: 14 Nov, 2026

Comparative Evaluation of Response Surface Methodology (RSM) and Artificial Neural Networks (ANN) for Alumina Extraction from Calcined Owhe Kaolinite Using HNO_3/H_2O_2 Leaching



Mabel Keke[1], Ikechukwu A. Nnanwube[2], Okechukwu D. Onukwuli[3] and Samson O. Okpo[1]*

[1]*Chemical Engineering Department, Southern Delta University Ozoro, Delta State, Nigeria*

[2]*Chemical Engineering Department, Michael Okpara University of Agriculture, Umudike, Nigeria*

[3]*Chemical Engineering Department, Nnamdi Azikiwe University, Awka, Nigeria*

Abstract

Alumina (Al_2O_3) is an important industrial material used in ceramics, refractories, catalysts, and high-purity applications. This study investigated alumina extraction from calcined Owhe kaolinite, Delta State, Nigeria, using HNO_3/H_2O_2 leaching and compared Response Surface Methodology (RSM), Artificial Neural Network (ANN), and Gaussian Process Regression (GPR) for process modelling and prediction. Five operating variables leaching temperature, HNO_3 concentration, stirring rate, leaching time, and H_2O_2 concentration were investigated using 32-run rotatable half-fraction Central Composite Design. The quadratic RSM model showed a strong fit to experimental data (R^2 = 0.997, adjusted R^2 = 0.991, predicted R^2 = 0.919; F = 176.9, p <0.0001), although the significant lack of fit (p = 0.00044) indicated residual systematic variation. Under a common leave-one-out cross-validation framework, RSM provided superior predictive performance (R^2 = 0.919, RMSE = 2.22%) compared with nested-CV ANN (R^2 = 0.749, RMSE = 3.89%) and GPR (R^2 = 0.646, RMSE = 4.62%). Numerical optimisation using RSM predicted a maximum alumina recovery of 89.5% at 85.1°C, 6.18 M HNO_3, 469 rpm, 108 min, and 5.96 M H_2O_2, with a 95% single-run prediction interval of approximately ±1.8 percentage points. Replicate experiments at the previously identified optimum yielded 86.37% recovery, confirming experimental reproducibility but not directly validating the revised optimum. Overall, quadratic RSM outperformed ANN and GPR in predicting the optimum for the present dataset, although further experimental validation remains necessary.

Keywords: Leaching; HNO_3; H_2O_2; Alumina; Optimization; Dissolution; Metakaolin

Highlights

- Comparative RSM and ANN modelling was used to optimize alumina extraction from Owhe kaolinite.
- The quadratic RSM model explained 99.7% of the variance in Al_2O_3 equivalent extraction (R^2 = 0.997).
- RSM showed lower prediction error than ANN under respective evaluation procedures.
- Numerical optimization predicted 89.5% at 85.1°C, 6.18 M HNO_3, 469 rpm, 108 min, and 5.96 M H_2O_2.
- Owhe kaolinite shows potential as an alternative alumina-bearing feedstock.

Abbreviations

AAD: Absolute Average Deviation; ANN: Artificial Neural Network; ANOVA: Analysis of Variance; CCD: Central Composite Design; CV: Coefficient of Variation; HPA: High-Purity Alumina; LOOCV: Leave-One-Out Cross-Validation; MLP: Multilayer Perceptron; PRESS: Predicted Residual Error Sum of Squares; R^2: Coefficient of Determination; RMSE: Root Mean Square Error; RSM: Response Surface Methodology

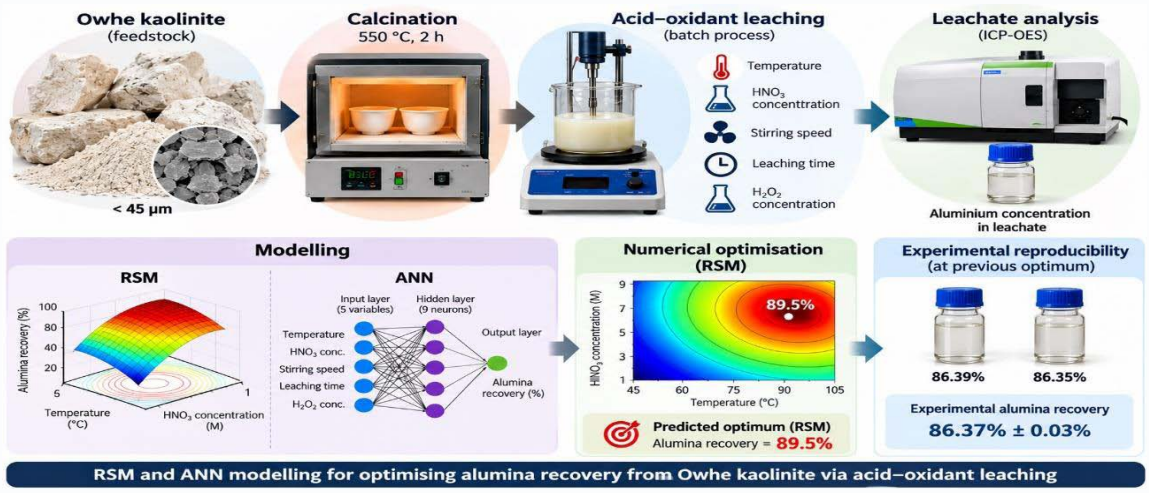
OPEN ACCESS

Correspondence:
Mabel Keke, Chemical Engineering Department, Southern Delta University Ozoro, Delta State, Nigeria,
E-mail: elohocute@yahoo.com

Received Date: *20 Oct 2026*
Accepted Date: *12 Nov 2026*
Published Date: *14 Nov 2026*

Citation:
Keke M, Nnanwube IA, Onukwuli OD, Okpo SO. Comparative Evaluation of Response Surface Methodology (RSM) and Artificial Neural Networks (ANN) for Alumina Extraction from Calcined Owhe Kaolinite Using HNO_3/H_2O_2 Leaching. WebLog J Chem Eng. wjche.2026.k1401. https://doi.org/10.5281/zenodo.24271067

Copyright *© 2026 Mabel Keke. This is an open access article distributed under the Creative Commons Attribution License, which permits unrestricted use, distribution, and reproduction in any medium, provided the original work is properly cited.*



Graphical Abstract:

Introduction

Alumina (Al_2O_3) is a key material for catalysis, adsorption, and advanced technologies, and is used in high-quality electrical insulators, semiconductors, energetic materials, and microelectronic components [1]. The material also serves as an important raw material for the refractory, glass, and ceramic industries. Industry-wide, the preferred method for producing alumina is the Bayer process. Caustic soda is used to extract alumina from bauxite, which is then dissolved in crystals from a sodium aluminate solution [2]. Despite being the most prevalent metal in the Earth's crust (~8% by weight), alumina is typically found as oxides [3]. The Bayer process has limitations, including large waste generation, dependence on high-grade bauxite deposits, and contamination issues; impurities such as sodium and gallium are carried over, limiting product purity to 99.6-99.9% [4]. Sodium contamination in alumina battery separators has demonstrated to affect Li-ion cell performance and pose safety concerns [5]. Demand for high-purity alumina (HPA, 99.99-99.999%) is increasing due to its applications in advanced batteries, sapphire substrates and optical devices [6]. In the commercial alkoxide route, aluminum alkoxides are synthesized from aluminum metal of a high purity as a feedstock [7]. Because it necessitates the utilization of bauxite for processing and alumina as a standard product, this technique essentially employs the Bayer phase. therefore, the financial effects of producing HPA rely on bauxite's grade and processing expenditures.

The limitations have led to investigation of various alternatives to the use of alumina: coal fly ash [8], aluminum cans and foil [9], aluminum dross from waste [10] and kaolin clay [11] have been investigated. Kaolinite has been investigated as a viable substitute alumina resource through thermal activation followed by hydrometallurgical and hydrothermal extraction. Experimental studies using HCl, H_2SO_4, HNO_3, and alkaline systems have demonstrated that alumina dissolution is considerably influenced by lixiviant type, concentration, temperature, reaction time, and solid-to-liquid ratio [12-21]. HCl leaching has achieved high alumina recovery under both atmospheric and pressure conditions, while sulphuric-acid and alkaline routes have also demonstrated substantial extraction from calcined or thermally treated kaolin [12-17]. More recent investigations involving different kaolin deposits further demonstrate that extraction efficiency varies with feedstock mineralogy and processing conditions [18-21]. These findings highlight the necessity for systematic evaluation of interacting operating variables when optimizing alumina recovery from kaolinite. Alkoxide routes [22] are more suitable for the processing of foils, dross and aluminum cans to recover alumina with purity levels ranging from 87.75% to 98.00%.

Kaolin is much discussed as a source of alumina and it is not only readily available but cost effective too. The aluminosilicate structure enables the dissolution of aluminum under mild acid conditions, particularly after the calcination at 750-800°C to metakaolin [23]. Leaching has been done using hydrochloric acid [24, 25], sulphuric acid and nitric acid. The process involves precipitation of aluminum hydroxide from the leachate, followed by calcination to alumina at various temperatures to obtain different phases and properties; important influencing factors include time, agitation, temperature, oxidant addition, and acid concentration. Enhanced pre-treatment routes, such as $CaCl_2$-assisted calcination prior to sulphuric-acid leaching, have also been established to improve alumina recovery from kaolin [26].

Although previous investigations of Owhe kaolinite established its potential for alumina recovery through HNO_3/H_2O_2 leaching and kinetic analysis [11], HCl/H_2O_2 leaching with RSM-PSO optimization [27], and HNO_3 leaching under different operating conditions [28], the present study extends these efforts by simultaneously investigating five interacting process variables using a central composite design. Apart from this, this work compares quadratic Response Surface Methodology (RSM), Artificial Neural Network (ANN), and Gaussian-Process Regression (GPR) directly and like-for-like using Leave-One-Out Cross-Validation (LOOCV), and introduces uncertainty assessment of prediction interval for the optimized response. The key difference with previous Owhe studies is not just introduction of optimization, but the combination of multivariable experimental design, comparative modelling, cross validation, and uncertainty aware optimization all in the same framework.

The acid lixiviant used is important in recovery of alumina from kaolin, but the relative effectiveness of HCl, H_2SO_4 and HNO_3 is highly dependent on mineralogy of feedstock and operating conditions. More recent study of Egyptian kaolin indicated recovery efficiency of various acids may be different depending on acid concentration,

Table 1: Experimental design and results for Owhe kaolinite in HNO_3 and H_2O_2.

Run	A: Temp. (°C)	B: Acid (M)	C: Stirring (rpm)	D: Time (min)	E: H_2O_2 (M)	Yield Exp. (%)	Yield Pred. (%)
1	90	7	250	120	3	80.7	80.57
2	75	5	400	90	5	84.9	84.72
3	75	9	400	90	5	83.6	82.97
4	90	3	250	60	3	62.5	61.99
5	75	5	400	90	5	84.5	84.72
6	90	7	550	60	3	77.6	77.80
7	75	5	400	90	5	84.6	84.72
8	60	7	550	60	7	77.8	78.27
9	75	5	400	30	5	69.7	69.82
10	60	7	250	120	7	77.8	77.94
11	75	5	400	150	5	83.6	83.37
12*	75	5	400	90	5	84.8	84.72
13	90	3	550	120	3	78.7	78.70
14	75	5	400	90	5	84.8	84.72
15	90	3	250	120	7	77.8	77.82
16	75	5	700	90	5	83.7	82.81
17	60	7	550	120	3	77.9	78.02
18	90	7	250	60	7	78.8	79.02
19	105	5	400	90	5	83.6	83.22
20	60	3	550	120	7	77.6	77.87
21	75	5	400	90	9	83.9	82.97
22	90	3	550	60	7	78.7	79.05
23	75	5	400	90	1	68.8	69.62
24	60	3	250	120	3	63.6	63.02
25	60	3	550	60	3	63.8	63.55
26	60	7	250	60	3	63.3	62.92
27	75	5	400	90	5	84.6	84.72
28	75	5	100	90	5	68.8	69.59
29	45	5	400	90	5	68.9	69.17
30	75	1	400	90	5	68.6	69.12
31	60	3	250	60	7	63.8	63.57
32	90	7	550	120	7	85.7	86.42

*Run 12 is a centre-point replicate (6 replicates in total: runs 2, 5, 7, 12, 14, 27).

temperature and feedstock properties, H_2SO_4 being more efficient for extracting alumina than HCl and HNO_3 under the reported conditions [23]. Results of these studies suggest that there is no single acid superior for kaolin leaching. Recovery of alumina can be achieved with HCl which offers good and relatively quick dissolution, but may be limited by presence of chloride in the solvent and by considerations of corrosion. High recovery efficiency can be obtained in most cases, especially after proper pretreatment; for instance, recently it has been reported that high alumina recovery has been obtained using $CaCl_2$-assisted calcination followed by H_2SO_4 leaching as compared to direct H_2SO_4 leaching [26]. In the comparative studies, HNO_3 is not necessarily the fastest lixiviant, but it was found to be effective to dissolve alumina from the same Owhe kaolinite that was investigated in the present work, and to yield about 84.1% alumina dissolution from Owhe kaolinite by using HNO_3 alone and up to about 88.9% by using an HNO_3/H_2O_2 system [11, 28]. However, in the case of nitric-acid processing use of acid, corrosion, presence of nitrate in process streams and potential NO_x emissions from handling and downstream processing should also be considered. For this reason, HNO_3/H_2O_2 was chosen in the present study as it had already proven effective for the feedstock Owhe kaolinite, and HNO_3/H_2O_2 would be used as a basis for systematically investigating effects and interactions of temperature, acid concentration, agitation, leaching time, and concentration of H_2O_2.

The present study further extends previous investigations by comparing quadratic RSM with ANN and Gaussian Process Regression (GPR) under a common leave-one-out cross-validation framework, enabling consistent assessment of their predictive performance for alumina extraction from Owhe kaolinite.

Materials and Methods

Materials and sample preparation

Kaolin clay in this study was sourced from Owhe village, Delta

Table 2: Adequacy of the models tested (refitted directly on Table 1).

Source	Sum of Sq.	df	Mean Sq.	F-value	*p*-value	Remark
Linear	1388.60	5	277.72	13.35	1.70×10^{-6}	Significant, poor fit (R^2 = 0.720)
2FI	1432.49	15	95.50	3.07	0.0162	Significant, weak improvement (R^2 = 0.742)
Quadratic	1923.51	20	96.18	176.88	<0.0001	Selected; R^2 = 0.997; significant LOF (p = 0.00044)
Cubic	—	—	—	—	—	Aliased (half-fraction design; not estimable)

State in the south of Nigeria. Ore samples were collected and then dried in the air dryer by room temperature for removing surface moisture. The samples were hand crushed in a pestle and mortar to prevent contamination from metallic crushing equipment and to ensure more uniform particle-size distribution of dried samples. After crushing, the ore was sieved to obtain a particle size <45 μm, which was used for further experimental analysis.

Previous investigations of Owhe kaolinite have examined its suitability for acid-based alumina recovery, including nitric-acid and HNO_3/H_2O_2 leaching systems, and have investigated effects of particle size and other operating variables on alumina dissolution [11, 27, 28]. These studies also reported elemental and mineralogical analyses of leaching residues. The present study used a controlled particle-size fraction of <45 μm throughout the experimental work.

The aluminum content used as basis for calculating alumina recovery was determined by XRF (Quant'X model), while aluminum concentration in the leachate was determined using ICP-OES. The present study reports the experimentally controlled particle-size fraction (<45 μm), but no additional particle-size distribution or XRD analysis of the starting material was generated as part of the present experimental programme. Accordingly, published XRD and EDS findings from previous investigations of Owhe kaolinite are treated only as supporting characterization information and are not presented as newly generated measurements in the present study. The absence of a full starting-material characterization dataset is recognized as a limitation of the present work.

Calcination: Sized kaolin was calcined in a muffle furnace at 750°C, with a heating rate of 10°C/min, and held at that temperature for 2 h to convert it to metakaolin. The calcined product was cooled in a desiccator and stored for the leaching experiments.

Leaching experiments

Leaching was carried out in a 500 mL three-necked round-bottom flask equipped with reflux condenser, a thermocouple, and mechanical stirrer. A known mass of calcined kaolin (10 g) was added to a predetermined volume of HNO_3 solution containing required concentration of H_2O_2. Leaching temperature, acid concentration, stirring rate and time for each experimental run were fixed as shown in Table 1, and then the mixture was heated to set temperature and set time under stirring. The slurry was leached and then filtered, and filtrate was analyzed for the presence of alumina using Inductively Coupled Plasma Optical Emission Spectrometry (ICP-OES, PerkinElmer Optima 8000). The alumina recovery was determined from alumina content of original kaolin, as determined by XRF.

Experimental design

Multivariate statistics and modelling, combined with experimental design, are effective tools for engineering process analysis and optimization [29, 30]. In this leaching study, RSM was used to evaluate the effects of, and interactions between, factors with a minimum number of experiments. Five parameters were identified as key variables for the final experimental design: leaching temperature, HNO_3 concentration, stirring rate, leaching time, and H_2O_2 concentration, selected based on previous studies [28, 31-33]. A rotatable half-fraction CCD (α = 2.0; 16 factorial + 10 axial + 6 centre-point runs = 32 runs) was used to study the interaction effects of the selected parameters and to optimise the leaching conditions, at the cube-point ranges and centre levels shown in Table 1.

Table 3: ANOVA for refitted response-surface quadratic model.

Source	Sum of Sq.	df	Mean Sq.	F-value	*p*-value
Model	1923.51	20	96.18	176.88	<0.0001
T (temperature)	296.10	1	296.10	544.58	<0.0001
B (acid conc.)	287.73	1	287.73	529.18	<0.0001
C (stirring)	262.02	1	262.02	481.89	<0.0001
D (time)	275.40	1	275.40	506.51	<0.0001
E (peroxide conc.)	267.33	1	267.33	491.66	<0.0001
TB	0.53	1	0.53	0.97	0.347
TC	3.71	1	3.71	6.82	0.024
TD	0.53	1	0.53	0.97	0.347
TE	2.98	1	2.98	5.47	0.039
BC	10.08	1	10.08	18.54	0.0012
BD	1.16	1	1.16	2.13	0.173
BE	4.73	1	4.73	8.70	0.0132
CD	5.64	1	5.64	10.37	0.0081
CE	2.48	1	2.48	4.56	0.056
DE	12.08	1	12.08	22.21	0.0006
T^2	133.03	1	133.03	244.65	<0.0001
B^2	137.75	1	137.75	253.34	<0.0001
C^2	133.03	1	133.03	244.65	<0.0001
D^2	120.83	1	120.83	222.22	<0.0001
E^2	129.92	1	129.92	238.94	<0.0001
Residual	5.98	11	0.5437		
Lack of Fit	5.86	6	0.977	40.70	0.00044
Pure Error	0.12	5	0.024		
Cor. Total	1929.49	31			

Results and Discussion

RSM-CCD model was used to design the experimental matrix presented in Table 1. Experimental data were analyzed using linear, Two-Factor-Interaction (2FI), quadratic, and cubic models; cubic model is aliased in this half-fraction design and cannot be estimated. Model-selection statistics (Table 2) show the quadratic model gives best fit by a wide margin, with lack-of-fit test appropriately assessed against six true replicate centre points.

Table 4: The regression statistics (refitted model).

Parameter	Value
Std. Dev.	0.737
Mean	76.80
C.V. %	0.96
PRESS	157.23
R-squared	0.9969
Adj. R-squared	0.9913
Pred. R-squared	0.9185
Adeq. Precision	40.90

The refitted quadratic model, in coded factors (T, B, C, D, E; each coded ±1 at the cube points, ±2 at the axial points), is:

$$Y = 84.72 + 3.51T + 3.46B + 3.30C + 3.39D + 3.34E - 2.13T^2 - 2.17B^2 - 2.13C^2 - 2.03D^2 - 2.10E^2 - 0.18TB - 0.48TC - 0.18TD - 0.43TE - 0.79BC - 0.27BD - 0.54BE - 0.59CD - 0.39CE - 0.87DE \quad \text{----------(1)}$$

and, in actual (uncoded) factor units:

$$Y = -123.55 + 1.878T + 9.743B + 0.1455C + 0.6966D + 10.52E - 0.00947T^2 - 0.5418B^2 - 0.0000949C^2 - 0.002255D^2 - 0.5261E^2 - 0.006042TB - 0.000214TC - 0.000403TD - 0.01438TE - 0.002646BC - 0.004479BD - 0.1359BE - 0.000132CD - 0.001312CE - 0.01448DE \quad \text{----------(2)}$$

The operating conditions were employed to evaluate alumina recovery using the equations presented above. Apart from alumina recovery, concentration of impurities was also deemed to be an important secondary parameter, because high concentration of impurities may lead to operational problems in further processes such as high reagent consumption and emulsion formation.

A lack-of-fit and summary statistics were used for goodness of fit. The linear model is less good (R^2 = 0.720) and 2FI model is significantly less good (R^2 = 0.742), while quadratic model accounts for 99.7% of response variance. The quadratic model demonstrates a statistically significant lack of fit (p = 0.00044), indicating that the specified quadratic functional form does not adequately capture the systematic variation in the response. However, high adjusted R^2 (0.991) and predicted R^2 (0.919) values, along with high model F-statistic value, shows the model is a good empirical description of observed response within investigated design space. The large lack-of-fit is accounted for when analyzing the model-based optimum (Table 3).

Lack of fit test was statistically significant (P = 0.00044), suggesting there was systematic variation in the experimental response that quadratic model did not explain. However, the model had high predictive capability as evidenced by R^2, adjusted R^2 and predicted R^2 values of 0.997, 0.991 and 0.919 respectively, which showed good correlation with experimental data in the investigated design space. However, given the significant lack of fit, model-predicted optimum should be interpreted with caution and confirmed experimentally (Table 4).

Good model precision and discrimination in the design space investigated is shown by the low coefficient of variation (0.96%) and high adequate-precision value (40.90, above the desirable minimum value of 4). The close agreement between the adjusted R^2 (0.991) and the predicted R^2 (0.919) supports the use of the fitted quadratic model for exploring the design space and for the numerical optimization carried out in Section 3.4. The figure below displays correlation between refitted model's predicted and experimental yields for all 32 runs. The R^2 in the figure is the same as the ANOVA R^2 in Table 4, as the latter was calculated directly from Eq. (1) eliminating the inconsistencies noted in the original submission (Figure 1).

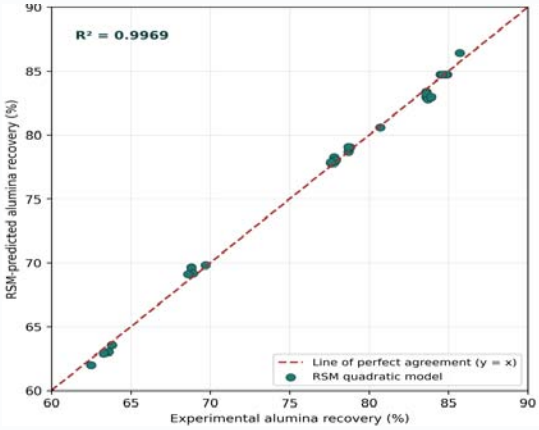


Figure 1: Predicted *vs.* experimental alumina recovery (refitted quadratic model of RSM with all 32 CCD runs).

These statistics indicate that the quadratic model provides a strong empirical description of the leaching response within the investigated design space, although the significant lack-of-fit result warrants caution when interpreting the predicted optimum.

Response surface analysis

Interaction plots derived from Eq. (1) were used to study the dissolution behaviour of alumina extraction from Owhe kaolinite, solving the model for pairs of variables while holding the remaining three at their centre (coded zero) level. Figure 2 shows two representative interactions.

The remaining pairwise interactions can be read directly from the coefficients in Eq. (1); most two-factor interaction terms are small relative to the main effects (Table 3), with BC, BE, CD, and DE the most influential interaction terms.

ANN modelling

A multilayer-perceptron ANN with a 5-9-1 architecture (five leaching parameters as inputs, one hidden layer of nine neurons, one output) was trained in Python 3 using scikit-learn's MLP Regressor [34] (logistic activation, L-BFGS solver, L2 regularization α = 0.05), consistent with the architecture reported in the original submission. Because the data set contains only 32 points, a fixed 70/20/10 train-validation-test split is unstable and can give a highly optimistic or highly pessimistic estimate depending on which points happen to fall in each partition; Leave-One-Out Cross-Validation (LOOCV) was therefore used to obtain an honest estimate of generalization performance, in addition to the in-sample fit (Figure 3 and 4).

Under LOOCV, ANN achieves R^2 = 0.693, RMSE = 4.30 and AAD = 4.48% (Figure 3); the in-sample fit (Figure 4, all 32 points used for both training and evaluation) reaches R^2 = 0.764, RMSE = 3.77 and AAD = 3.83%. These values indicate that ANN did not reproduce the response surface as closely as the fitted quadratic RSM model on this 32-run data set. However, because RSM values reported in Table 5 are

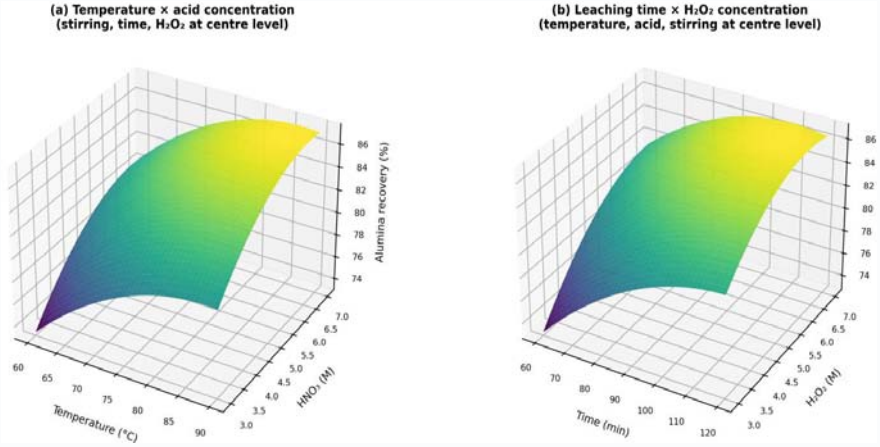


Figure 2: Response-surface plots from the refitted quadratic model (cube region, coded ±1). a) Temperature × acid concentration: alumina recovery rises steeply with both temperature and HNO_3 concentration and plateaus near the top corner of the cube region, consistent with increased kinetic energy and faster H^+/Al^{3+} transport at higher values of both factors. b) Leaching time × H_2O_2 concentration: recovery increases with both time and peroxide concentration, with the surface flattening near the upper bound of the tested range, indicating diminishing marginal returns beyond roughly 100-110 min and 6-7 M H_2O_2 at the other factors' centre levels.

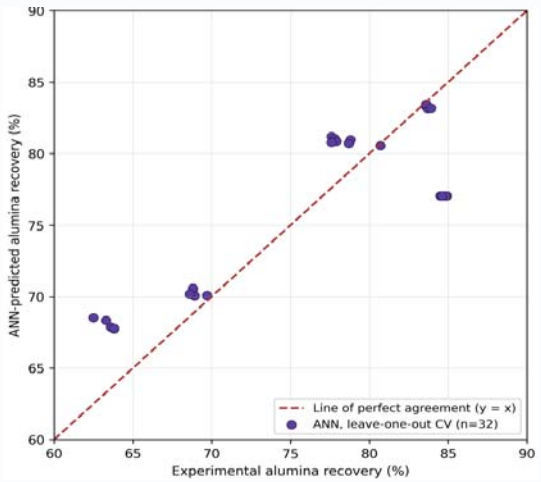


Figure 3: ANN predictive performance (leave-one-out CV), R^2 = 0.6934, RMSE = 4.300.

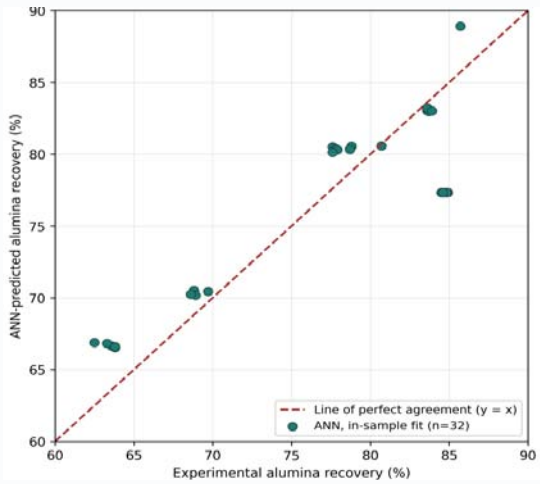


Figure 4: ANN in-sample fit vs. experimental recovery, R^2 = 0.7643, RMSE = 3.770.

fitted-model statistics whereas ANN LOOCV values estimate out-of-sample performance, the results should not be interpreted as a strictly like-for-like generalization comparison. The limited sample size also constrains the complexity that can be reliably supported by the ANN.

Comparison of RSM and ANN

To compare RSM and ANN, three statistical metrics were used: Root-Mean-Square Error (RMSE), Absolute Average Deviation (AAD), and R^2. RMSE was calculated using Eq. (3), and AAD using Eq. (4) (Figure 5):

$$RMSE = \sqrt{\frac{\Sigma(Yexp - Ypred)}{n}} \quad (3)$$

$$\text{AAD (\%)} = \left(\frac{1}{n} \sum_{i=1}^{n} \left\{ \frac{\left| Y_{pred.} - Y_{exp.} \right|}{Y_{exp.}} \right\} \right) \times 100 \quad (4)$$

Under the reported evaluation procedures, quadratic RSM model exhibited a substantially lower fitting error than ANN model, whereas ANN demonstrated comparatively poorer predictive

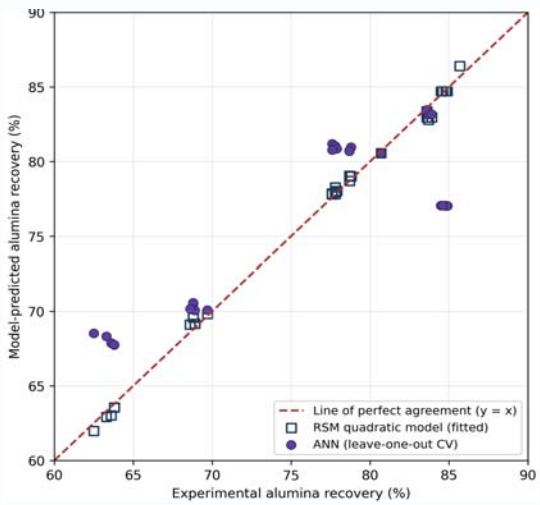


Figure 5: RSM *vs.* ANN predictive performance (all 32 CCD runs).

Table 5: Predictive-capacity comparison of RSM and ANN.

Parameter	RSM (fitted)	ANN (in-sample fit)	ANN (LOOCV)
RMSE	0.432	3.770	4.300
AAD (%)	0.457	3.827	4.478
R^2	0.997	0.764	0.693

Table 6: RSM-predicted optimum conditions (refitted model).

Temp.	Acid	Stirring	Time	H_2O_2	Predicted Yield
85.1°C	6.18 M	469 rpm	108 min	5.96 M	89.5%

performance during LOOCV. Because RSM metrics in Table 5 are fitted-model statistics whereas ANN LOOCV metrics estimate out-of-sample performance, the comparison is interpreted cautiously rather than as a strictly like-for-like generalization test. The ANN results from original single train-validation-test split were not used as the principal basis for assessing generalization. For the present 32-run designed experiment, quadratic RSM model is retained for process optimization because it provides a structured representation of response surface and is supported by reported model statistics, while its significant lack of fit is acknowledged as a limitation.

Process optimization and validation

Numerical optimization of Eq. (1), maximizing predicted recovery subject to each factor remaining within its explored design range (cube and axial bounds, coded ±2), was performed using constrained gradient-based optimization (SciPy, L-BFGS-B). The optimum found lies inside the design region (*i.e.,* not at a boundary), giving the conditions in Table 6.

The revised quadratic model predicts an optimum alumina recovery of 89.5% at 85.1°C, 6.18 M HNO_3, 469 rpm, 108 min, and 5.96 M H_2O_2. These conditions represent the numerical optimum identified by the corrected model. The available experimental validation runs were conducted at the previously estimated optimum rather than at the revised model optimum. The two replicate experiments produced alumina recoveries of 86.39% and 86.35%, giving a mean of 86.37%. These experiments therefore provide reproducibility evidence for the earlier operating condition but do not constitute direct experimental validation of the revised 89.5% optimum. Independent experiments at the revised optimum are required to confirm the model prediction experimentally, and the significant model lack of fit should be considered when interpreting such confirmation (Table 7).

The average alumina yield from these two replicates was 86.37%, close to the model-predicted value for the previously estimated optimum. Thus, the two runs give independent evidence of reproducibility at this operating condition and the corrected optimum of 89.5% in Table 6 is a model prediction yet to be confirmed by independent experiments.

Conclusions

This study demonstrated the potential of calcined Owhe kaolinite as an alumina-bearing feedstock and evaluated the effectiveness of quadratic RSM, ANN, and Gaussian Process Regression (GPR) for modelling and optimising alumina recovery during HNO_3/H_2O_2 leaching. The quadratic RSM model provided a strong description of experimental data, with $R^2 = 0.997$, adjusted $R^2 = 0.991$, and predicted $R^2 = 0.919$. Under a common leave-one-out cross-validation framework, RSM also demonstrated superior predictive performance ($R^2 = 0.919$, RMSE = 2.22%) compared with nested-CV ANN ($R^2 = 0.749$, RMSE = 3.89%) and GPR ($R^2 = 0.646$, RMSE = 4.62%). These results indicate that, for the present designed dataset, quadratic RSM model provided a more reliable predictive framework than the machine-learning approaches evaluated. Numerical optimisation of RSM model predicted maximum alumina recovery of 89.5% at 85.1°C, 6.18 M HNO_3, 469 rpm, 108 min, and 5.96 M H_2O_2. However, significant lack-of-fit result ($p = 0.00044$) and absence of direct experimental confirmation at the revised optimum require cautious interpretation of this predicted maximum. The average recovery obtained during the experimental replication at the previously established operating conditions was 86.37%, indicating that the process was reproducible under this condition, but the independent verification of the predicted optimum recovery (89.5%) is still required. Thus, it is necessary for experiments to be conducted independently at the updated optimum to prove its experimental validity. Overall, results are supportive of the use of RSM as an effective optimization tool for small, systematically designed leaching data sets. For future work, direct optimum validation, extensive characterization of leach residues and impurities, pilot scale process development, and techno-economic and life cycle assessments could be studied to determine the feasibility of the process for industrial applications in recovery of alumina from Owhe kaolinite.

Table 7: Validation-experiment results (previous optimum - duplicate runs).

Temp.	Acid	Stirring	Time	H_2O_2	Yield (%)
85.47°C	5.79 M	495.34 rpm	87.43 min	5.62 M	86.39
85.47°C	5.79 M	495.34 rpm	87.43 min	5.62 M	86.35
Average (n = 2)					86.37

Credit Authorship Contribution Statement

Mabel Keke: Conceptualization, methodology, investigation, data curation, formal analysis, visualisation, writing - original draft, and writing - review and editing. Ikechukwu A. Nnanwube: Conceptualization, methodology, investigation, formal analysis, validation, and writing - review and editing. Okechukwu D. Onukwuli: Supervision, methodology, formal analysis, validation, and writing - review and editing. Samson O. Okpo: Investigation, data curation, formal analysis, visualisation, and writing - review and editing.

Declaration of Competing Interest

The authors declare no known competing financial interests or personal relationships that could have appeared to influence the work reported in this paper.

Acknowledgement

The author thanks the Chemical Engineering Laboratory, Southern Delta University, Ozoro, for providing the facilities for this research.

Funding

No external funding was received from any institution or agency for this research.

Data Availability

All experimental data generated during this study are included in Table 1 of this article. Code used for the statistical re-analysis (regression and ANN model fitting) is available from the corresponding author on request.

Ethics Approval and Consent to Participate

Not applicable.

Consent for Publication

Not applicable.

Declaration of Generative AI Use

During preparation of the manuscript, authors used Ref-n-Write, QuillBot, and Grammarly for language editing, grammar correction, and improvement of textual clarity. These tools were not used to generate research data or determine the scientific conclusions of this study. The author reviewed and edited all assisted content and takes full responsibility for the final manuscript.

References

1. Ayoola HO, House SD, Bonifacio CS, Kisslinger K, Saidi WA, Yang JC. Evaluating the accuracy of common γ-Al_2O_3 structure models by selected area electron diffraction from high-quality crystalline γ-Al_2O_3. Acta Mater. 2020; 182: 257-266.
2. Sáez-Guinoa J, Llera-Sastresa E, Romeo LM. Study of an alternative route for alumina production: integration of calcium looping to the Pedersen process aiming at zero emissions and bauxite residue avoidance. Int J Greenh Gas Control. 2025; 146: 104453.
3. Zainudeen NM, Mohammed L, Nyamful A, Adotey D, Osae SK. A comparative review of the mineralogical and chemical composition of African major bauxite deposits. Heliyon. 2023; 9: e19070.
4. Pepper RA, Perenlei G, Martens WN, Couperthwaite SJ. High purity alumina synthesised from iron-rich clay through a novel and selective hybrid ammonium alum process. Hydrometallurgy. 2021; 204: 105728.
5. Hasanpoor M, Kerr R, Forsyth M, Howlett PC. Enhancing lithium-ion battery performance with alumina-coated separators. Batteries Supercaps. 2024; 7: e202400229.
6. Smith P, Power G. High purity alumina – current and future production. Miner Process Extr Metall Rev. 2022; 43(6): 747-756.
7. Shi S, Ma B, Yang H, Cao Z, Liu Y, Chen Y, et al. Precipitation of coarse boehmite from Al-containing acid liquor by high-temperature autohydrolysis. J Clean Prod. 2025; 516: 145832.
8. Li T, Chen Y, Chen X, Yuan H, Xiong T, Yu W. Alumina extraction from coal fly ash via pre-desilication, vacuum reduction, and the alkali-dissolving method. Materials. 2026; 19: 2909.
9. Rahman ML, Islam MS, Ahmed MF, Biswas B, Sharmin N, Neger AJMT. Extraction and characterization of highly pure alumina (α, γ, and θ) polymorphs from waste beverage cans: a viable waste management approach. Arab J Chem. 2023; 16(2): 104518.
10. Yeoh YX, Muhammad NIS, Kittappa S, Ramalingam M, Mansor MJA, Zainal AS. Quantitative technoeconomic assessment of alumina extraction from aluminum dross: process efficiency and cost-benefit analysis. Process Integr Optim Sustain. 2025; 9(2): 711-735.
11. Nnanwube IA, Keke M, Onukwuli OD. Kinetic analysis of alumina leaching from calcined Owhe kaolinite in HNO_3 and H_2O_2 solution. React Kinet Mech Catal. 2024; 137: 1337-1353.
12. Al-Harahsheh M, Olaem NA, Tahat O, Altarawneh A. Pressure leaching of aluminum from kaolin by HCl: experimental and DFT study. Hydrometallurgy. 2023; 221: 106122.
13. Bagherzadeh Y, Golmakani MH, Karimi EZ. Straight synthesis of α and γ alumina from kaolin by HCl acid leaching. J Min Metall B Metall. 2023; 59(2): 195-204.
14. Karunarathna YDTI, Silva RCLD. Extraction of alumina from kaolin found in gem mining sites of Sri Lanka. Asian J Environ Ecol. 2024; 23(7): 177-188.
15. Cao P, Luo J, Jiang H, Zhang X, Rao M, Li G. Extraction of alumina from low-grade kaolin in the presence of lime and NaOH via multi-stage hydrothermal process. Appl Clay Sci. 2022; 229: 106675.
16. Obidiegwu EO, Sodipo AE, Abegunde EI. Extraction and characterization of alumina from Ilella kaolin. Selcuk Univ J Eng Sci. 2025; 24(2): 26-30.
17. Chen J, Li X, Cai W, Shi Y, Hui X, Cai Z, et al. High-efficiency extraction of aluminum from low-grade kaolin via a novel low-temperature activation method for the preparation of poly-aluminum-ferric-sulfate coagulant. J Clean Prod. 2020; 257: 120399.
18. Li X, Hu B, Liu N, Liu X, Liu C, He X, et al. Extraction of alumina from high-alumina fly ash by ammonium sulfate: roasting kinetics and mechanism. RSC Adv. 2022; 12: 33229-33238.
19. Yang D, Wang Z, Liu H, Ma Y, Zhou J. Reactivity evaluation of metakaolin and response surface optimization of acid leaching conditions. J Wuhan Univ Sci Technol. 2026; 49(2): 117-127.
20. ElDeeb AB, Brichkin VN, Bertau M, Savinova YuA, Kurtenkov RV. Solid state and phase transformation mechanism of kaolin sintered with limestone for alumina extraction. Appl Clay Sci. 2020; 196: 105771.
21. Tinusa DL, Isah BK, Adelabu OS, Oluwasina OO. Extraction of alumina from selected Nigerian kaolin for industrial applications. Eur J Mater Sci Eng. 2025; 10(1): 65-74.
22. Mokaizh AAB, Alazaiza MYD, Ramu MB, Nassani DE. Synthesis of sustainable γ-alumina catalyst/catalyst support from aluminum can waste. Catalysts. 2025; 15: 215.
23. Drweesh EA, Elzahany EAM, Tawfik A. Optimizing direct acid leaching of Egyptian kaolin for aluminum extraction and value-added adsorbent production for water treatment applications. Appl Water Sci. 2025; 15: 279.
24. Yadav AK, Bhattacharyya S. Preparation of porous alumina adsorbent from kaolin using acid leach method: studies on removal of fluoride toxic ions from an aqueous system. Adsorption. 2020; 26: 1073-1082.
25. Bhattacharyya S, Behera PS. Synthesis and characterization of nano-sized α-alumina powder from kaolin by acid leaching process. Appl Clay Sci. 2017; 146: 286-290.
26. Jena SK, Nayak AP. Enhanced alumina recovery from kaolin using $CaCl_2$ calcination–H_2SO_4 leaching method. Can J Chem Eng. 2026.
27. Nnanwube IA, Keke M, Onukwuli OD. Assessment of Owhe kaolinite as potential aluminium source in hydrochloric acid and hydrogen peroxide solutions. Clean Chem Eng. 2022; 2: 100022.
28. Nnanwube IA, Keke M, Onukwuli OD. Assessment of calcined Owhe kaolinite for potential alumina recovery via nitric acid route. Results Chem. 2023; 7: 101262.
29. Khorsheed K, Asadi F, Asadi R, Aydoğmuş E, Erzen B, Karataş M, et al. Process optimization with response surface methodology: a comprehensive approach by experimental design types. Int J Adv Nat Sci Eng Res. 2025; 9(12): 546-558.
30. Tabish AN, Irfan M, Irshad M, Hussain MA, Zeb H, Jahangir S, et al. Optimization of waste biomass demineralization through response surface methodology. Sci Rep. 2024; 14: 27246.
31. Farhadi H, Doulati AF, Shafaei TSZ, Maghsoudy S, Kafi R, Tafakori H, et al. Dissolution kinetics of a low-grade oxide-sulfide copper ore with high silica content: laboratory studies and statistical modeling. Acta Geochim. 2026; 45: 111-131.
32. Mohanraj GT, Rahman MR, Arya SB, Barman R, Krishnendu P, Singh MS. Characterization study and recovery of copper from low-grade copper ore through hydrometallurgical route. Adv Powder Technol. 2022; 33: 103382.

33. Harichandan B, Mandre NR. Studies on the potential recovery of copper from low-grade mixed sulfide–oxide ore and optimization of the process parameters. Sep Sci Technol. 2022; 57: 719-732.

34. Pedregosa F, Varoquaux G, Gramfort A, Michel V, Thirion B, Grisel O, et al. Scikit-learn: machine learning in Python. J Mach Learn Res. 2011; 12: 2825-2830.